

Hepatic mitochondrial SAB deletion or knockdown alleviates diet induced metabolic syndrome, steatohepatitis and hepatic fibrosis

Sanda Win^{1,2}, Robert W.M. Min³, Jun Zhang⁴, Gary Kanel^{1,5}, Brad Wanken⁶, Yibu Chen⁷, Meng Li⁷, Ying Wang⁸, Ayako Suzuki⁸, Filbert W.M. Aung⁹, Susan F. Murray¹⁰, Mariam Aghajan¹⁰, Tin A. Than^{1,2}, Neil Kaplowitz^{1,2}

Supporting Materials and Methods

Supporting References

Supporting Tables

Supporting Figures and Figure legends

Supporting Materials and Methods

Reagents and antibodies

Antisera to JNK (9252), P-JNK (4668), PHB1 (2426), SEK1/MKK4 (3346), Phospho-SEK1/MKK4 (Ser257; 4514), P-Akt (S473; 4060), Akt (pan) (4691), c-Src (2109), P-p38 (4511), total p38 (8690), P-AMPK (2535), AMPK α (2532), P-PDH α 1 (inactive) (S293; 31866), ATF2 (35031) were purchased from Cell Signaling Technology. Total JNK (JNK 1/2/3) (sc-571; Santa Cruz biotechnology), CPT1A (SAB2100476; Sigma Aldrich), GAPDH (G9295; Sigma Aldrich), β -actin (A3854; Sigma Aldrich), OTC (HPA000243; Atlas), HADHA (ab54477; Abcam), Col-1 α (ab34710; Abcam), P-ATF2 (ab32019; Abcam) were used. Affinity purified antisera to SAB which recognizes C-terminus of SAB was purchased from Abbomax (#630-490) and characterized in previous publications. Fructose, sucrose, etomoxir, oligomycin, CCCP, rotenone, pyruvate, glucose, octanoate and insulin were purchased from Sigma-Aldrich. Tat-D-JNKi (JNKi-peptide) was

purchased from MedChem Express. Tat-Sab_{KIM1} (SAB-peptide) was purchased from Neo Peptide.

Mice and diet

Male C57BL/6NHsd mice were purchased from Envigo and bred to obtain littermates. Eight weeks old cage littermates were used for experiments. *Sab^{ff}* mice (C57BL/6NHsd strain) were generated as described previously. *Sab^{ff}* mice were crossbred with *Alb-Cre^{ERT2}* mice (*Alb^{tm1}(cre/ERT2)Mtz*), provided by Pierre Chambon (Institut de Genetique et de Biologie Moleculaire et Cellulaire, Strasbourg, France) to generate tamoxifen-inducible hepatocyte-specific *Sab*-knockout mice (*Sab^{ΔHep}*). Mice were crossbred with *Sab^{ff}* mice for more than 20 generations. *Sab^{ff}* and *Sab^{ΔHep}* mice (age 6-8 weeks) were fed with tamoxifen supplemented diet (Envigo) for one week. After an additional week of chow diet, mice were fed high-fat high-calorie fructose (HFHC) diet which was reported to induce murine NAFL/NASH. HFHC diet (Research Diet #D12331) provides 5.56 kcal/g: 58% of calories from fat (93% from fully hydrogenated coconut oil which is highly rich in medium chain saturated fat without trans-fat, and 7% from soybean oil which is rich in poly/mono-saturated fat, ie. all fat are saturated); 26% of calories from carbohydrate (mainly from sucrose & maltodextrin) of which 6.5% is from fructose; 16.4% of calories from protein. No cholesterol was supplemented. Drinking water was supplemented with fructose (fructose (55%) 23.1g/L and sucrose (45%) 18.9g/L); total 168 Calorie/42 g/L. Chow diet (PicoLab Rodent diet #5053) provides 4.11 kcal/g: 13% of calories from fat, 62% of calories from carbohydrate (0.24% of calories is from fructose), 25% of calories from protein, and trace amount of cholesterol. Other cohorts of wild type mice fed of HFHC

for various times received treatments with *Sab-ASO* or *GalNAc-Sab-ASO* compared to scrambled control ASOs. All experiments were performed using cage littermates. All mouse-diet feeding started at 8 weeks of age. Studies were performed in male mice as females are resistant to NAFL/NASH. All animal procedures were conducted utilizing protocols and methods approved by the Institutional Animal Care and Use Committee and were in compliance with Animal Welfare Act and NIH Guide for the Care and Use of Laboratory Animals.

Serum assays and Multiplex Assays

Blood for glucose was collected through tail-capillary for time course analyses. Blood for serum separation was collected through dorsal vein during sample collection at the time of euthanization. Serum alanine aminotransferase (ALT) was measured by Alanine Aminotransferase (ALT or SGPT) Activity Colorimetric /Fluorometric Assay Kit (Biovision). Blood glucose was measured by ACCU-CHEK nano (Roche). Serum levels of cytokines, insulin and peptide hormones, were determined by MILLIPLEX MAP Mouse cytokine/chemokine, adipokine, adiponectin, myokine using Immunology Magnetic Bead Panel. Immunology Multiplex Assays were analyzed according to the manufacturer's instructions (Millipore Sigma).

Metabolic tolerance tests

Basal blood glucose levels were determined after overnight fasting for 16 hours. Glucose tolerance test (GTT) was performed as follows: overnight fasted mice received D (+)

glucose 1mg/g body weight dissolved in PBS ip. Blood glucose was measured before glucose injection and 15, 30, 60, 120 min after glucose injection.

Metabolic phenotyping

Animals were housed under specific pathogen-free conditions, maintained in a temperature (20-22°C) controlled room and 30-70% relative humidity (RH) with a 12 h light/dark cycle, and provided *ad libitum* access to water and diet. Body Composition Analysis: Whole body mass, fat mass and lean mass was analyzed by nuclear magnetic resonance using the EchoMRI 700 Body Composition Analyzer (EchoMRI, Houston, TX) on the same day as the energy expenditure measurement. Fat mass is defined as the mass of all the fat in the body expressed as equivalent weight of canola oil. Lean mass is defined as the mass of all body parts containing water, excluding fat, bone minerals, and substances which do not contribute to the NMR signal, such as hair, claws, etc. All organs including liver contribute to lean mass. However, it is important to note that contribution of liver to lean mass decreased and shifted to fat mass as liver accumulated fat, especially in massive enlarged fatty liver at 30 weeks and 52 weeks of HFHC diet feeding. EE measurement: Mice were acclimated in the home cage system (PhenoMaster/ LabMaster home cage System, TSE Systems) for 24 hours followed by 72 hours data collection period. O₂ consumption and CO₂ production were measured to determine the respiratory exchange ratio (RER) and energy expenditure (EE) by indirect calorimetry method. Food intake and locomotor activity (XY) were determined continuously throughout the study. Metabolic measurements were performed at the Rodent Metabolic Core of Children's Hospital of Los Angeles. Analysis of EE: average EE of each mouse (kcal/hour) is plotted

with whole body mass, lean mass, or fat mass and depicted as regression plot and as residual EE.⁽¹⁾ Statistical significance ($p < 0.05$) was determined by Analysis of Covariance (ANCOVA) and shown as (*).

Isolation of steatotic-hepatocytes and measurement of respiration

Wild type male mice were fed the HFHC diet for 12 weeks. Steatotic hepatocytes (steatotic PMH) were isolated by collagenase perfusion and differential centrifugation and seeded on collagen coated Seahorse cell culture plates at 2.5×10^4 cell per well in DMEM high glucose with 10%FBS. Soon after attachment of PMH, dead and unattached cells were washed out with seeding medium and attached cells were kept in medium overnight. Steatotic PMH were rinsed with serum free, glucose/pyruvate free, low amino acid XF medium pH 7.2 for 5 times and set into Seahorse XF analyzer at 37°C as described in our previous publications. The program was set to equilibrate at 37°C for 5min before measurement of basal oxygen consumption rate (OCR), and then $5 \mu\text{M}$ of Tat-SAB_{KIM1} peptide (SAB peptide) or Tat-D-JNKi peptide (JNKi peptide) was introduced through injection ports. Second injection was programmed set at 9 hours after the first injection. OCR was acquired throughout 18 hours, and then oligomycin was injected at a final concentration of $1 \mu\text{g/ml}$ and then CCCP was injected at a final concentration of $20 \mu\text{M}$. The oligomycin inhibitable respiration represents ATP generating-oxidative-phosphorylation. CCCP-induced OCR was defined as the maximal respiratory capacity of mitochondria. When required, measurements were normalized to the average of the measured points of the basal (starting) level of OCR of each well. Error bars in one representative experiment represent S.D of 5 wells. Statistical significance ($P < 0.05$)

between peptide treatment versus no treatment was analyzed by two ways ANOVA and indicated as (*). Experiments were repeated 3 times with separate cell preps from separate mice. Data was analyzed in groups of wells from each preparation.

Western Blot Analysis

Aliquots of protein extracts were fractionated by electrophoresis on 7.5, 10, or 4-20% SDS-polyacrylamide gel (Bio-Rad). Subsequently, proteins were transferred to nitrocellulose membrane using iBlot transfer (Invitrogen), and blots were blocked with 5% (w/v) nonfat milk dissolved in Tris-buffered saline with Tween 20. The blots were then incubated with the primary and secondary antibodies and detected by luminol ECL reagent (Thermo Scientific) using film or ChemiDoc (Bio-Rad). All gels shown are representative samples from at least three experiments. Densitometry was performed from 3 separate experiments using NIH image J software.

Detection of protein oxidation

Proteins are one of the major targets of oxygen free radicals and other reactive species.⁽²⁾ As a consequence of oxidative modification, carbonyl groups are introduced into proteins at lysine, arginine, proline or threonine residues in a site-specific manner and can be derivatized to 2,4-dinitrophenylhydrazone (DNP-hydrazone) by reaction with 2,4-dinitrophenylhydrazine (DNPH). The DNP-derivatized protein samples are separated by 4-20% SDS-PAGE and detected by Western blotting using specific antibody as described in OxyBlot assay kit (#S7150, Millipore). β -actin immunoblot appeared as a strong broad band on OxyBlot membrane and it was not suitable to use as loading control for

quantitation. As an alternative, PHB1 immunoblot was used as a loading control because PHB1 level does not vary in our model and appeared as a sharp single band.

siRNA transfection and ATF2-KO cell lines

HEK293 cells (ATCC) were transfected with 10 μ M siRNA targeting to ATF2 (siATF2; Ambion) using Lipofectamine RNAiMAX transfection reagent. >90% knockdown was achieved at 72 hours after transfection. 48 hours after transfection cells were split into dishes and rested overnight, cells were then treated with BSA or palmitic acid (PA-BSA) 250 μ M for 24 hours. 3 separate experiments were performed.

The ATF2-KO AML12 cell line was generated by polybrene 10 μ g/ml mediated transfection of lentivirus delivering sgRNA targeting to ATF2 with Cas9 co-expression (all-in-one CRISPR/Cas9 from Applied Biological Materials Inc.). The KO cell line was selected with puromycin. AML12 cells with lentivirus mediated stable expression of Cas9 were used as control. ATF2-KO cells were cultured and grown in the same conditions as wild type cells. Cells were treated with DMSO or tunicamycin (Tm) 5 μ g/ml in serum free medium for 24 hours.

Adeno-associated virus mediated ATF2 knockdown

ATF2 depletion in hepatocytes in vivo was performed by delivery of AAV8.TBG.ATF2-RNAi.eGFP (Penn vector core, UPenn). ATF2-RNAi targets to GGAGCCTTCTGTTGTAGAAAC and was designed as a miRNA. GFP alone was used as a control vector. After 12 weeks of HFHC diet feeding mice were injected into tail vein with 5 $\times 10^{12}$ GC (ddTiter) AAV8.TBG.ATF2-RNAi.eGFP or GFP and continue the HFHC

diet for 4 weeks. 4 weeks after injection, livers and blood were harvested. Tissue lysates were prepared for immunoblotting.

Quantitation of mRNA

Total RNA was extracted using a RNeasy RNA extraction kit (Qiagen). 0.5 µg of total RNA was reverse transcribed using an Omniscript reverse transcription kit (Qiagen) supplemented with 10 µM random hexamer (Applied Biosystems). The resulting cDNA (volume equivalent to 5–10 ng of total RNA in a reverse transcription reaction) was subjected to quantitative real-time PCR analysis with the SYBR Green PCR master mix (Qiagen) and ABI Prism 7900HT sequence detection system (Applied Biosystems). The relative quantification of mRNA expression was analyzed by the standard curve method following the manufacturer's instructions (Applied Biosystems). Three pairs of primers (TATCAACCGACGGGAGACTGA & TGCCAGTTCGTCTAGTTTCAC; AAACCTAGA CGAACTGGCAAAGAA & AAACCTGCCGCTTGTCATCCT; AAATGCTGAACCATGCT ACTCA & TCCTTGTGTACTAGCTCACTCC) were used to determine mouse *Sab* mRNA level. Data were analyzed using the SDS2.4 software (Applied Biosystems). *Sab* mRNA was normalized to endogenous *Tbp* expression. Primers for SREBP target genes were obtained from Primer Bank (<https://pga.mgh.harvard.edu/primerbank/>).

SAB (SH3BP5) expression analysis of human transcriptome data and datamining

Hepatic *SAB* expression was analyzed using microarray data of 23 male NAFLD patients enrolled in the Duke University Health System NAFLD Biorepository (Duke University, Durham, NC). The data analysis was approved by Duke University Institutional Review

Board. Of 24 men in this study, one case with cirrhosis was excluded from the analysis. 23 male patients were assessed for associations between SAB and histologic severity of NAFLD. Histological grades were defined according to NASH CRN Criteria: (1) NASH is defined as the presence of any degree of hepatocyte ballooning ≥ 1 or lobular inflammation ≥ 2 ; (2) Fibrosis severity was defined as mild fibrosis (F0-F1) and advanced fibrosis (F3). Student's *t*-test or Welch's *t*-test if heteroscedasticity was detected was used to compare SAB expression levels between non-NASH versus NASH or between mild versus advanced fibrosis. Spearman correlation analysis was applied to detect the monotonic correlation between SAB expression levels versus NAS overall score and subcategories. $p < 0.05$ is statistically significant.

SAB expression in microarray data sets (GSE63067, E-MEXP-3291, GSE24807, GSE15653, GSE61260) and RNA-seq data was analyzed using data-mining platforms: BaseSpace Space Correlation Engine⁽³⁾ (Illumina Inc., San Diego, CA, USA, <https://www.nextbio.com/>) and Ingenuity Pathway Analysis Analysis Match (QIAGEN Inc., <https://www.qiagenbioinformatics.com/products/ingenuity-pathway-analysis>). $p < 0.05$ indicates that differential expression of SAB in NASH or obesity versus normal healthy control was significant.

Histological grading of NASH activity score (NAS score)

NASH Activity Score (NAS) in mice studies was defined according to⁽⁴⁾: Steatosis grade "0" = < 5%, "1" = 5-33%, "2" = 34-66%, "3" = > 66%; Portal inflammation grade "0" = none to minimal, "1" = greater than minimal; Lobular inflammation grade "0" = none, "1" = < 2 per 20x field, "2" = 2-4 per 20x field, "3" = > 4 per 20x field; Hepatocellular ballooning "0"

= none, “1” = few/probable, 2 = many/definite. NAS score ≥ 5 was defined as NASH. The scoring was performed by a pathologist (G.K) in coded fashion without knowledge of the treatment.

In-situ hybridization of *SAB (SH3BP5)* RNA in human liver

Human liver samples (de-identified) were obtained from Samsara Sciences. Samples were scored for NAS, and three normal and three NASH liver sections underwent in-situ hybridization by Advanced Cell Diagnostics (ACD) using probe Hs-SH3BP5 (Cat. No.515779) (RNAscope). Semi-quantitative scoring was performed based on the number of dots per cell rather than the signal intensity (score “0” = <1 dot /cell, “1” = 1-3 dots /cell, “2” = 4-9 dots /cell, “3” = 10-15 dots /cell, “4” = >15 dots /cell).⁽⁵⁾

RNA-seq for gene expression analysis

Liver samples were collected around 11am on sample collection days without changing the feeding schedule and samples were snap-frozen in RNA-*later* RNA stabilizing solution. Gene expression transcriptome analysis was performed by NGS RNA-sequencing provided by Qiagen sequencing core. RNA was isolated from snap frozen tissue using the miRNeasy Mini Kit (QIAGEN) according to the manufacturer’s instructions with an elution volume of 45 μ l. The library preparation was done using TruSeq® stranded total RNA sample preparation kit with rRNA depletion (Illumina inc). Briefly, the starting material of total RNA (100 ng) was rRNA depleted using biotinylated, target-specific oligos combined with Ribo-Zero rRNA removal beads. The isolated RNA was subsequently fragmented using enzymatic fragmentation. Then, the first strand

synthesis and second strand synthesis were performed and the double stranded cDNA was purified (AMPure XP, Beckman Coulter). The cDNA was end repaired, 3' adenylated, and Illumina sequencing adaptors ligated onto the fragment ends, and the library was purified (AMPure XP). The RNA stranded libraries were pre-amplified with PCR and purified (AMPure XP). The size distribution of the libraries was validated and quality inspected on a 4200 TapeStation (Agilent Technologies). High quality libraries were pooled in equimolar concentrations based on the Bioanalyzer automated electrophoresis system (Agilent Technologies). The library pools were quantified using qPCR and the optimal concentration of each library pool was used to generate the clusters on the surface of a flow cell before sequencing on a NextSeq500 instrument (2x75 cycles) according to the manufacturer instructions (Illumina Inc.). The analysis of RNA-seq data was conducted using the RNA-seq workflow with Partek Flow software (v9. Partek Inc., St. Louis, MO, USA). Briefly, the raw sequencing reads were first subjected to sequencing quality score-based trimming (Phred QC ≥ 20 , min read length =25 nt) before alignment to the mouse genome build mm10 using Star 2.73a (Dobin et al. 2013) with default settings. Gencode M24 mouse transcriptome annotation (Mudge and Harrow 2015) was then used to quantify the aligned reads using the Partek E/M method. Finally, gene level read counts in all samples were normalized using the Upper Quartile method (Bullard et al. 2010) and subjected to differential expression analysis using the Partek Gene Specific Analysis method (genes with fewer than 10 aligned reads in any sample among a data set were excluded). The differentially expressed gene (DEG) lists were generated using the cutoff of FDR < 0.05 and fold changes greater than 1.5, either up or down.

Subsequent functional analysis of the DEG lists was carried out using the Ingenuity Pathway System (Qiagen, Redwood City CA).

Histology and immunohistochemical staining

Livers were fixed in 10% buffered formalin, embedded in paraffin, and cut into 5- μ m thick sections. Specimens were stained with hematoxylin/eosin and Sirius red. Sections of frozen livers were stained with Oil Red-O. Immunohistochemical staining was performed on formalin fixed paraffin embedded tissue sections using specific antibodies for CD45 (Invitrogen (eBioscience) 14-0451-82), CD68 (Abcam ab125212), MPO (ab9535), F4/80 (ab6640), TNF (ab6671) and α -SMA (ab5694), and color developed by DAB substrate.

Image analysis of area of fibrosis

10X magnification of histology photomicrographs from Sirius red stained tissue sections without counter staining of nucleus were analyzed with Image-J software (Fiji) for area of staining, representing the area of fibrosis. Briefly, at constant brightness and image dimension, red stained fibrosis area was digitally adjusted to saturated level excluding nuclei. The area of red-saturation and the area of the image were measured.

Antisense oligonucleotides (ASO)

ASO were provided by Ionis Pharmaceuticals either as standard MOE-ASO or GalNAc-linked MOE-ASO. *Scrambled control* (CCTTCCCTGAAGGTTCTCC) and *Sab ASO* (GCTGCCGCTACAGGGAATGC) were used as described before (31,33). ASO was dissolved in sterile PBS and oligonucleotide concentration was determined before

aliquoting for storage at -80°C . Mice were treated with 2.5 mg/kg of GalNAc-*Sab/control-ASO* or 25-50 mg/kg of standard *Sab/control-ASO* or scrambled controls ip three times per week. Samples were collected one day after the last injection. The 50 mg/kg dose schedule was based on prior work showing it reduced SAB protein to extremely low levels. The 25 mg/kg and 2.5mg/kg were selected based on preliminary data showing moderate knockdown to attempt to blunt the HFHC diet induced large increase in SAB protein expression in order to approximate normal level observed in chow fed mice.

Supporting References

1. Corrigan JK, Ramachandran D, He Y, Palmer CJ, Jurczak MJ, Chen R, et al; Mouse Metabolic Phenotyping Center Energy Balance Working Group, Banks AS. A big-data approach to understanding metabolic rate and response to obesity in laboratory mice. *Elife* 2020;9:e53560.
2. Meakin PJ, Chowdhry S, Sharma RS, Ashford FB, Walsh SV, McCrimmon RJ, et al. Susceptibility of Nrf2-null mice to steatohepatitis and cirrhosis upon consumption of a high-fat diet is associated with oxidative stress, perturbation of the unfolded protein response, and disturbance in the expression of metabolic enzymes but not with insulin resistance. *Mol Cell Biol.* 2014;34:3305-3320.
3. Kupersmidt I, Su QJ, Grewal A, Sundaresh S, Halperin I, Flynn J, et al. Ontology-based meta-analysis of global collections of high-throughput public data. *PLoS One* 2010;5:e13066.
4. Kleiner DE, Brunt EM, Van Natta M, Behling C, Contos MJ, Cummings OW, et al; Nonalcoholic Steatohepatitis Clinical Research Network. Design and validation of a histological scoring system for nonalcoholic fatty liver disease. *Hepatology* 2005;41:1313-1321.
5. Wang F, Flanagan J, Su N, Wang LC, Bui S, Nielson A, et al. RNAscope: a novel in situ RNA analysis platform for formalin-fixed, paraffin-embedded tissues. *J Mol Diagn* 2012;14:22-29.

Table S1

	Human Liver sample type	FC	p value	Case (n)	Control (n)	Publication
1	NASH vs Normal control	1.40	4.5E-02	9	7	PLoS One. 2015;10(5):e0124544.
2	NASH vs Normal control	1.46	2.8E-03	9	19	Drug Metab Dispos. 2011;39(10):1954-1960.
3	NASH vs Normal control	2.72	7.0E-06	12	5	Pathology. 2015;47(4):341-348.
4	Obesity (no DM) vs Lean control	1.61	6.0E-04	3	5	J Clin Endocrinol Metab. 2009;94(9):3521-3529.
5	Obesity/NAFL vs Normal control	1.25	3.6E-03	38	38	Proc Natl Acad Sci U S A. 2014;111(43):15538-15543.
6	PHH (in vitro liver model): Free fatty acid with High glucose+Insulin vs Low glucose+Insulin	2.32	9.8E-17	8	9	JCI Insight. 2016;1(20):e90954.

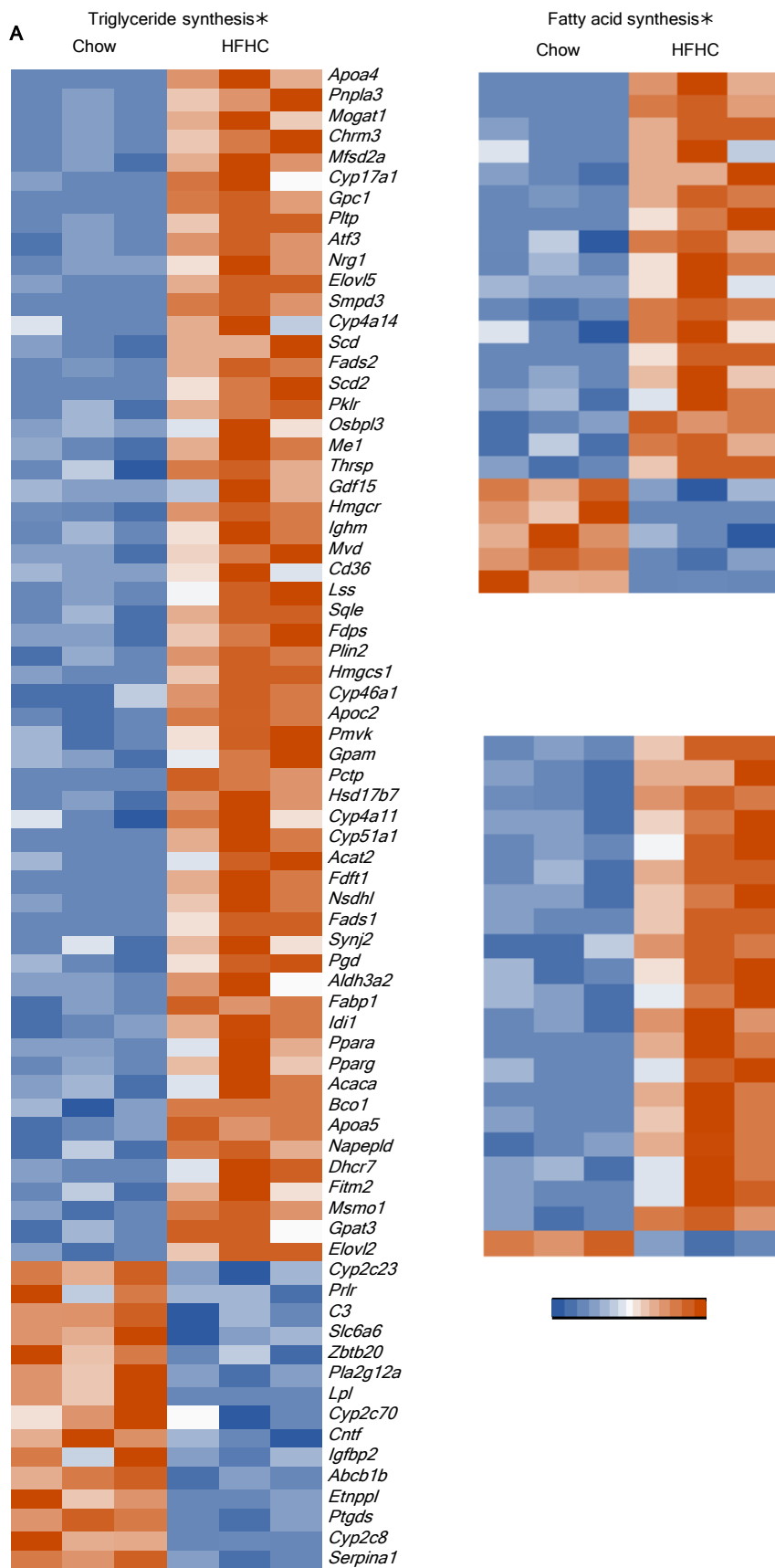
Table S1. Data mining of *SAB (SH3BP5)* expression using BaseSpace Correlation Engine (BSCE) and Ingenuity Pathway Analysis (IPA). Data sets of human NASH vs normal control (n=3 data sets, microarray), obesity vs normal control (n=2 data sets, microarray), human primary hepatocytes (n=1 data set, RNA-seq) studies were examined. The fold change (FC) and statistical significance (*p* value) were obtained with BSCE (Data set #1-4, 6) and IPA (Data set #5). PHH = primary human hepatocyte

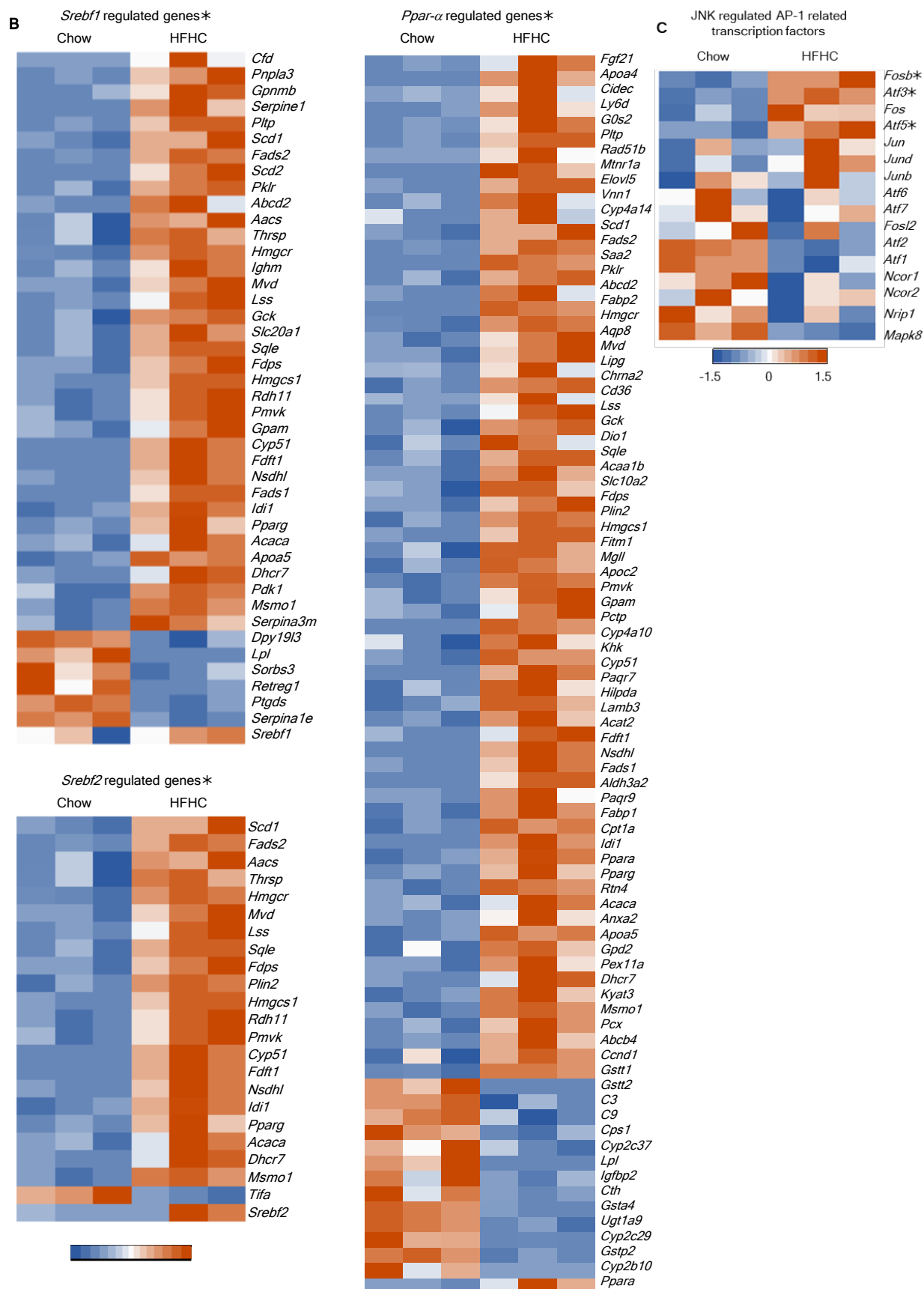
Table S2

Histology Outcome	Spearman Correlation Coefficient (r_s)	<i>P</i> value
NASH activity score *	0.52	0.0125
Steatosis *	0.43	0.0399
Inflammation(lobular) *	0.46	0.0320
Inflammation(portal)	0.30	0.1835
Ballooning hepatocyte	0.34	0.1149
Fibrosis	0.31	0.1430

Table S2. Correlation of histologic severity of NAFLD and *SAB (SH3BP5)* mRNA expression from microarray data of 23 male patients. Spearman correlation analysis was applied to detect the monotonic correlation between *SAB* expression and histology features. Significant correlation ($p < 0.05$) is shown as (*).

Figure S1





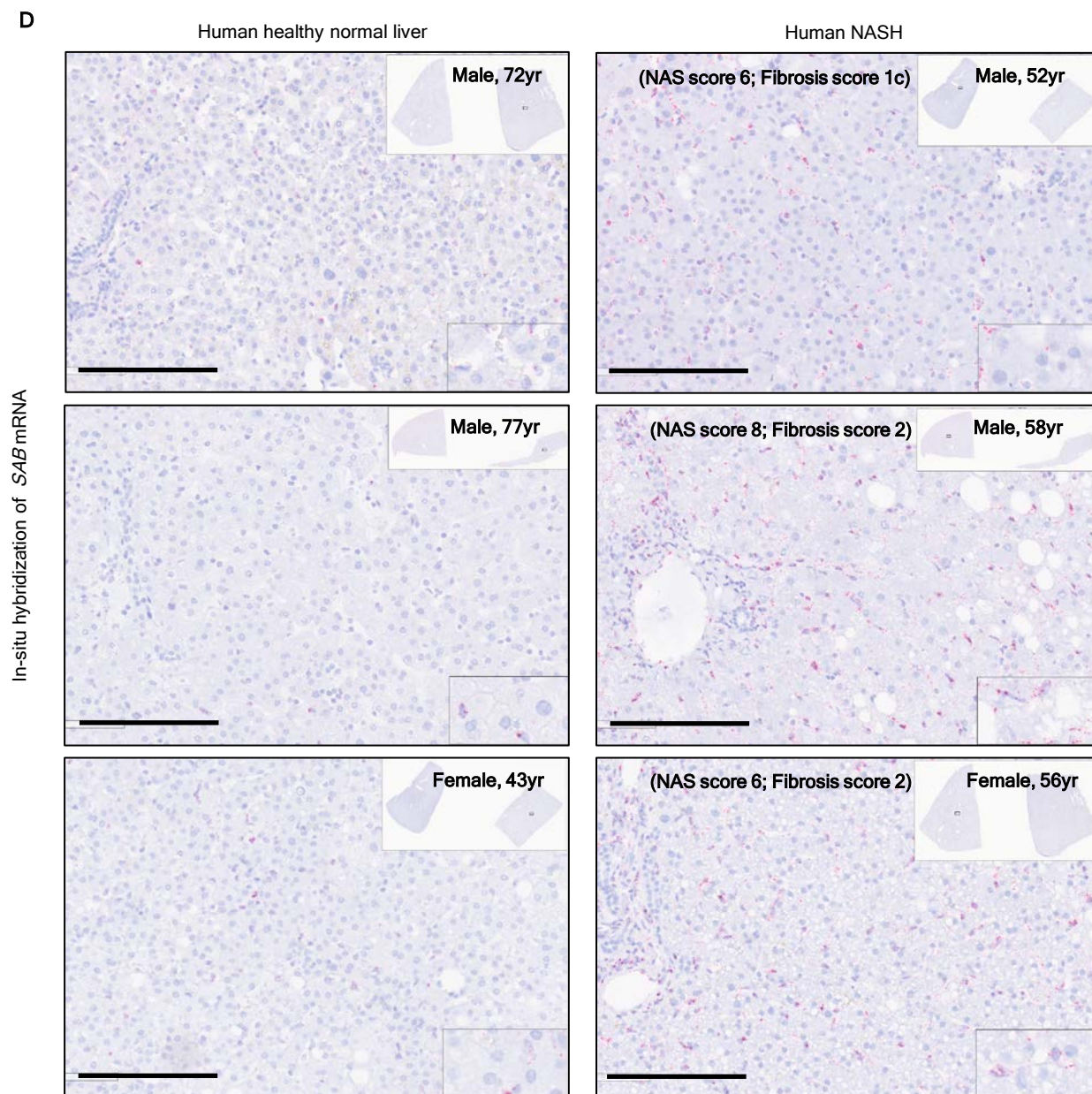


Fig. S1. Analysis of hepatic genes differentially regulated by HFHC diet in C57BL/6N wild type male littermates, *SAB* expression level in human NASH, and the regulation of *Sab* expression by ATF2 in cell lines. RNA-seq analysis was performed on three independent libraries prepared from 4-month-old C57BL/6N wild type male littermates fed chow or HFHC diet for 8 weeks (n=3 per group). Liver samples were

collected around 11am on the day of sample collection and snap-frozen in RNA-*later* RNA stabilizing solution. The differentially expressed genes (DEG) were generated by Partek Flow with the cutoff of FDR < 0.05; fold change \geq 1.5. The DEG list was analyzed using Ingenuity Pathway Analysis (IPA) which revealed that *de novo* lipogenesis/cholesterol synthesis pathways are not only significantly impacted but also substantially activated. Normalized counts of the key underlying DEGs for each pathway were standardized to a mean of zero and standard deviation to one, and then used to generate the heatmaps. **(A)** Genes related to triglyceride synthesis (z-score = 3.463, overlap *p*-value = 2.35E-18); fatty acid synthesis (z-score = 2.959, overlap *p*-value = 1.98E-05); cholesterol synthesis (z-score = 2.8, overlap *p*-value = 1.3E-16). **(B)** Upstream regulatory pathways significantly changed by HFHC diet vs chow are shown as heatmap: *Srebf1* (SREBP1) (z-score 4.513, overlap *p*-value 1.02E-26), *Srebf2* (SREBP2) (z-score 4.127, overlap *p*-value 1.11E-19) and *Ppar- α* (z-score 3.235, overlap *p*-value 2.77E-53) regulated pathway activation. The genes are listed with highest expression (*top*) to lowest expression (*bottom*) in livers of mice fed HFHC. **(C)** RNA expression of AP-1 mediated JNK regulated transcription factors is shown. A few JNK-target genes are significantly activated, but JNK pathway activation is not significantly changed at this early stage consistent with Fig.1A. (*=FDR < 0.05; fold change \geq 1.5). See GEO accession numbers (GSE154426). **(D)** Full size photomicrographs of in-situ hybridization of *SAB* (*SH3BP5*) mRNA in healthy and NASH human livers. n=3 per group. Scale bar = 200 μ m; Representative example of one is also shown in Fig.1E.

Figure S2

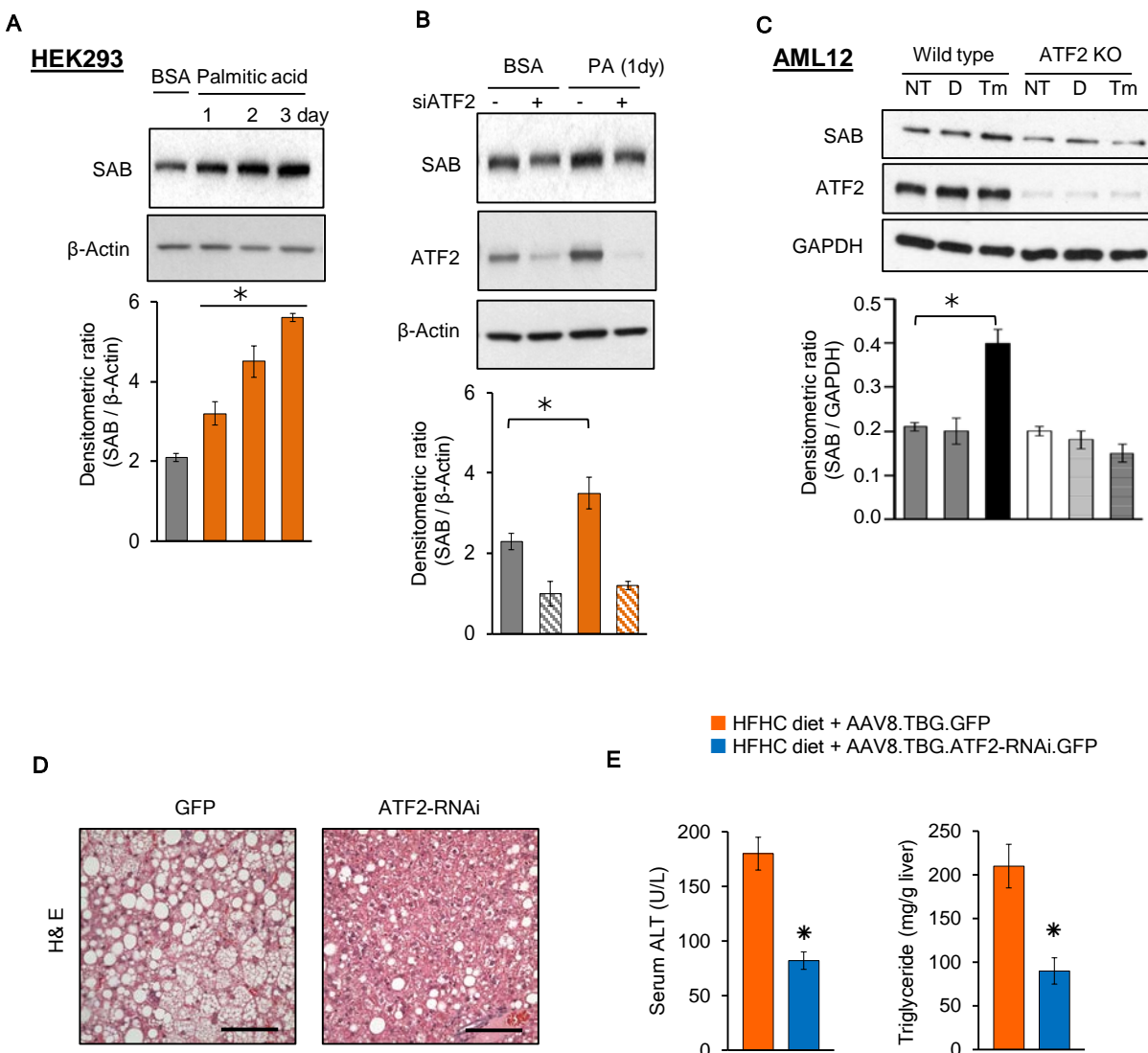


Fig. S2. ATF2 knockdown prevents diet induced SAB expression and JNK activation. (A) HEK293 cells were treated with BSA or palmitic acid (PA-BSA) 250 μ M for 3 days and SAB expression was determined. Representative image of 3 separate immunoblots. Bar graph shows densitometry of SAB levels $\ast=p<0.05$, unpaired 2-tailed Student's *t*-test. $n=3$ separate experiment. (B) HEK293 cells were transfected with 10 μ M siRNA targeting to ATF2 (siATF2; obtained from Ambion) using Lipofectamine RNAiMAX transfection reagent. 2 days after transfection cells were split and seeded overnight. Cells were then treated with BSA or palmitic acid (PA-BSA) 250 μ M for 24 hours. Protein lysate was collected and ATF2 and SAB levels were determined by immunoblot. Bar graph shows densitometry of immunoblots. $\ast=p<0.05$, unpaired 2-tailed Student's *t*-test. $n=3$ separate experiment. β -actin was used as loading control in all blots. (C) ATF-2 mediates ER stress induced SAB expression. ATF2-KO AML12 cells were cultured and grown in the same conditions as wild type cells. Cells were treated with tunicamycin (Tm) 5 μ g/ml in serum free medium for 24hr. Not treated [NT] and DMSO [D] were used as a vehicle controls. ATF2 and SAB levels were determined by immunoblot. Bar graph shows densitometry of the immunoblots. GAPDH, loading control. (D) Male wild type littermates were fed HFHC diet for 16 weeks. After 12 weeks of HFHC diet mice were given intravenous AAV8.TBG.GFP or AAV8.TBG.ATF2-RNAi and continued the HFHC diet for an additional 4 weeks, at which time the livers and blood were harvested. Liver histology: representative images of H&E staining liver sections of HFHC diet fed mice. Scale bar = 100 μ m. (E) Serum ALT and liver triglycerides. 5 mice/group, $\ast=p<0.05$, unpaired, 2-tailed Student's *t*-test.

Figure S3

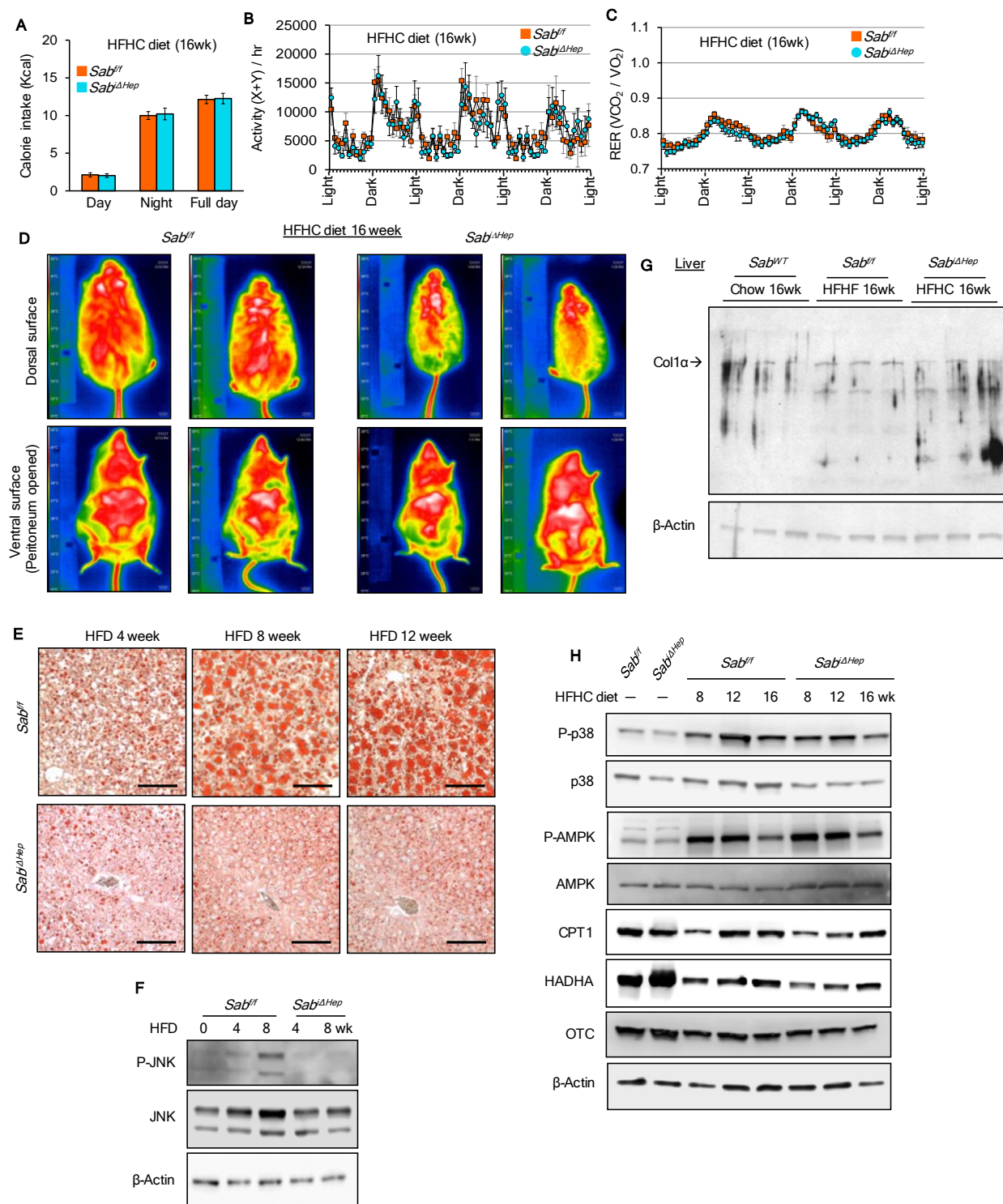
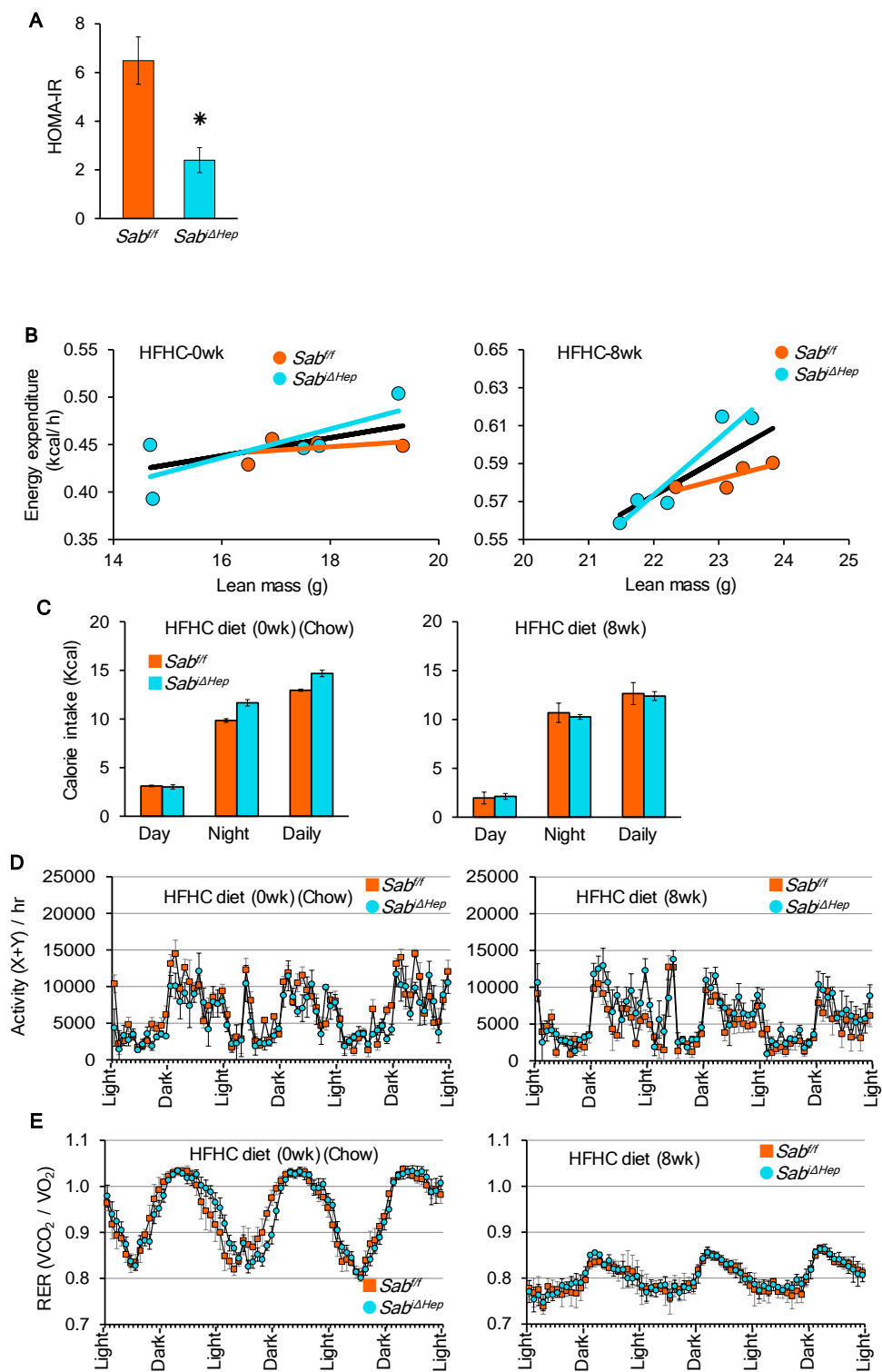


Fig. S3. Effect of deletion of hepatic *Sab* on diet-induced fatty liver. (A-D) Male wild type (*Sab^{ff}*) and hepatocyte specific *Sab* deleted (*Sab^{iΔHep}*) mice (at age 8 weeks) were fed with HFHC diet for 16 weeks. Body weight gain and food/drink intake were measured weekly. Calorie intake, locomotor activity and respiratory exchange ratio (RER) were examined by PhenoMaster/ LabMaster home cage System, TSE Systems. n=6 mice per group. Body heat was assessed using heat sensitive thermal camera on the dorsal surface and ventral surface (peritoneum opened) of anesthetized mice at room temperature. Surface temperature was estimated by color code from high to low: white, red, yellow, green, blue and black. Surface temperature per body surface area was not significantly different. (E, F) **Effect of hepatic deletion of *Sab* in HFD model (Western diet with 1% cholesterol). *Sab^{ff}* and *Sab^{iΔHep}* mice were fed with high-fat diet (16% protein, 58% saturated fat, and 26% carbohydrate) (DYET#180529) for 8 and 12 weeks. Liver Oil Red-O staining was performed at indicated times of diet feeding. Scale bar = 100μm. n=5 mice/group. Immunoblot demonstrates JNK activation was prevented in *Sab^{iΔHep}* mice at 4 and 8 weeks of HFD feeding. P-JNK activation was determined by specific antibody. (G,H) **Assessment of protein levels and activity in immunoblot of livers from chow and HFHC fed *Sab^{ff}* and *Sab^{iΔHep}* mice** using specific antibodies: Col1α, p38, P-p38, AMPK, P-AMPK (active). CPT1, HADHA, OTC. β-Actin is the loading control. Protein extracts (30 μg) from whole liver were used for each lane of immunoblots. Representative immunoblots from 3 separate experiments are shown.**

Figure S4



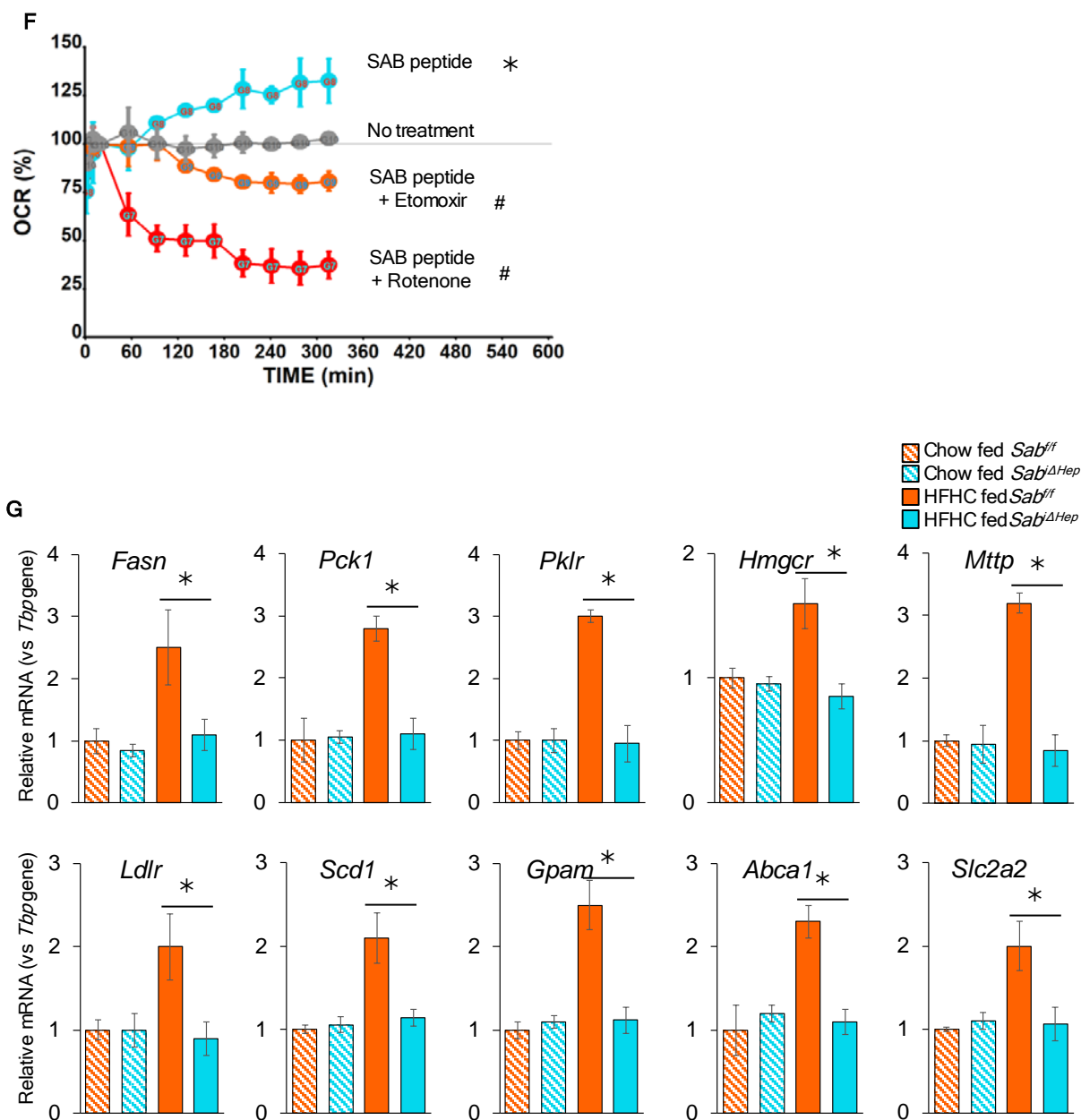
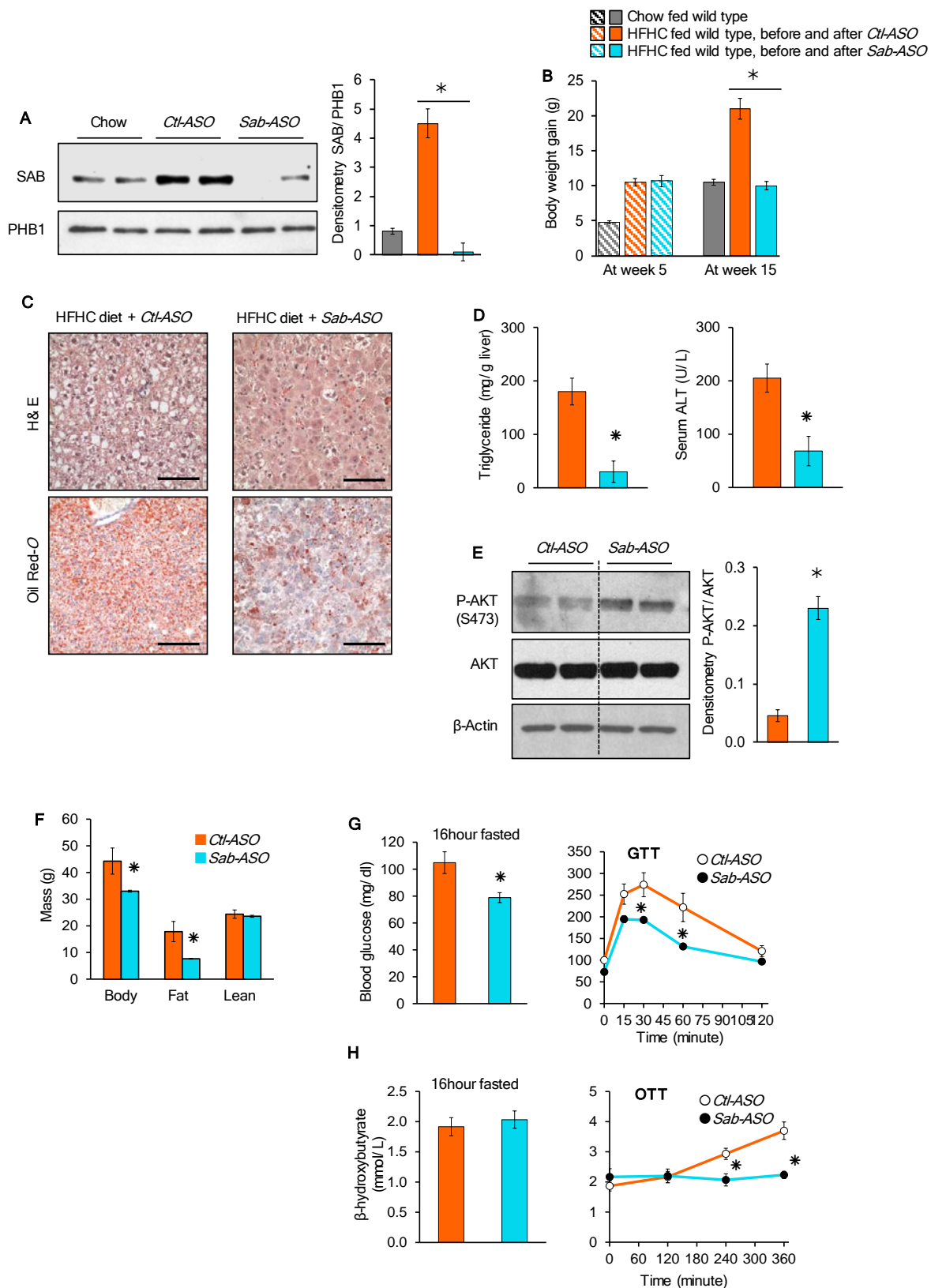


Fig. S4. Effect of deletion of hepatic *Sab* on energy metabolism and lipogenesis.

Male wild type (*Sab^{f/f}*) and hepatocyte specific *Sab* deleted (*Sab^{iΔHep}*) mice (at age 8 weeks) were fed the HFHC diet (A). Insulin resistance was calculated by HOMA-IR after 16 weeks of feeding. $n=5$ mice per group, $*=p<0.05$ *Sab^{iΔHep}* versus *Sab^{f/f}* by unpaired, 2-tailed Student's *t*-test. (B-E) Mice were fed HFHC diet for 8 weeks and metabolic

phenotyping was performed as described in the methods. n=5 mice per group. **(F)** Lipid metabolism of steatotic hepatocytes was examined by Seahorse XF analyzer. PMH were isolated from wild type C57BL/6N mice fed with HFHC diet for 12 weeks and seeded on collagen coated Seahorse cell culture plate. Before analysis, cells were rinsed and incubated in XF medium supplemented with glucose 1mM/ pyruvate 10 μ M. Cells were untreated or treated (via injection ports) with cell permeable Tat-SAB-peptide (SAB-KIM1 peptide) 10 μ M \pm etomoxir or rotenone. Oxygen consumption (OCR) was measured over a 5 hours time course. (n=3 separate experiment, $\ast = p < 0.05$ SAB peptide treatment versus no treatment; $\# = p < 0.05$ etomoxir with or without rotenone versus no treatment by two-way ANOVA. Data represents mean \pm SEM. **(G)** SREBPs target genes involved in lipogenesis at 16 weeks of HFHC diet feeding were determined by qPCR. n=5 mice per group, $\ast = p < 0.05$ by unpaired, 2-tailed Student's *t*-test.

Figure S5



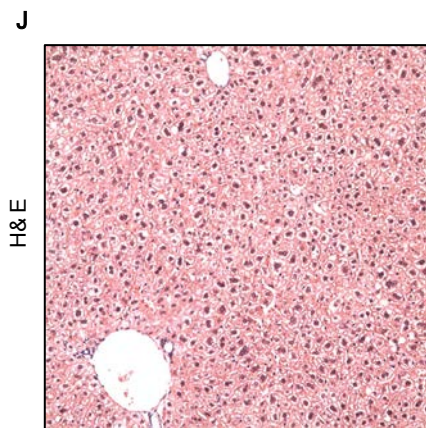
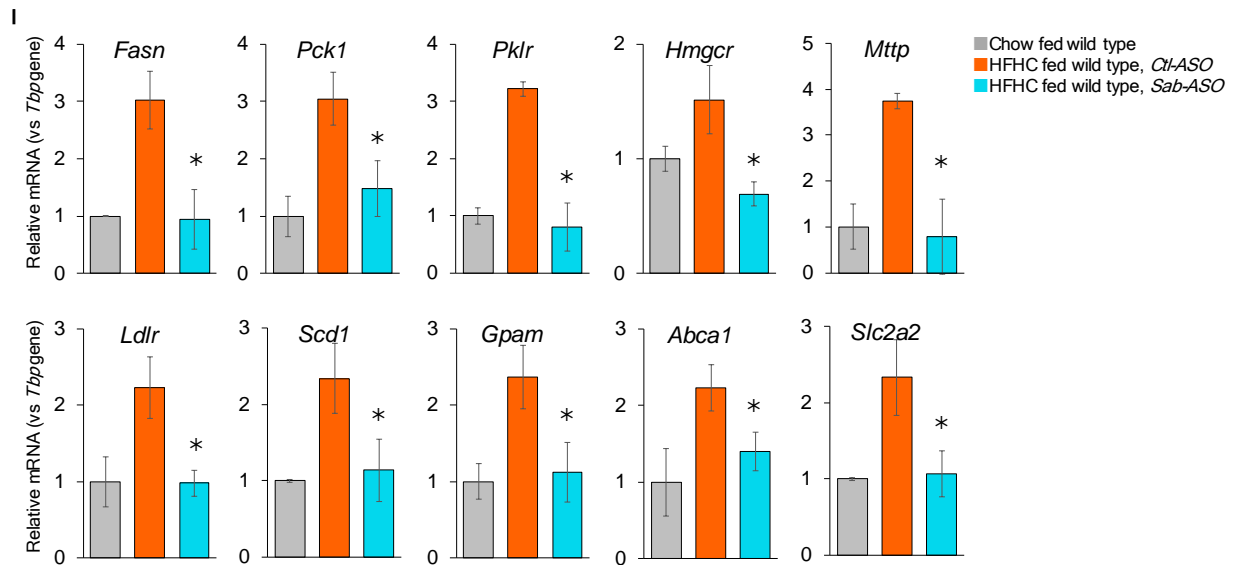
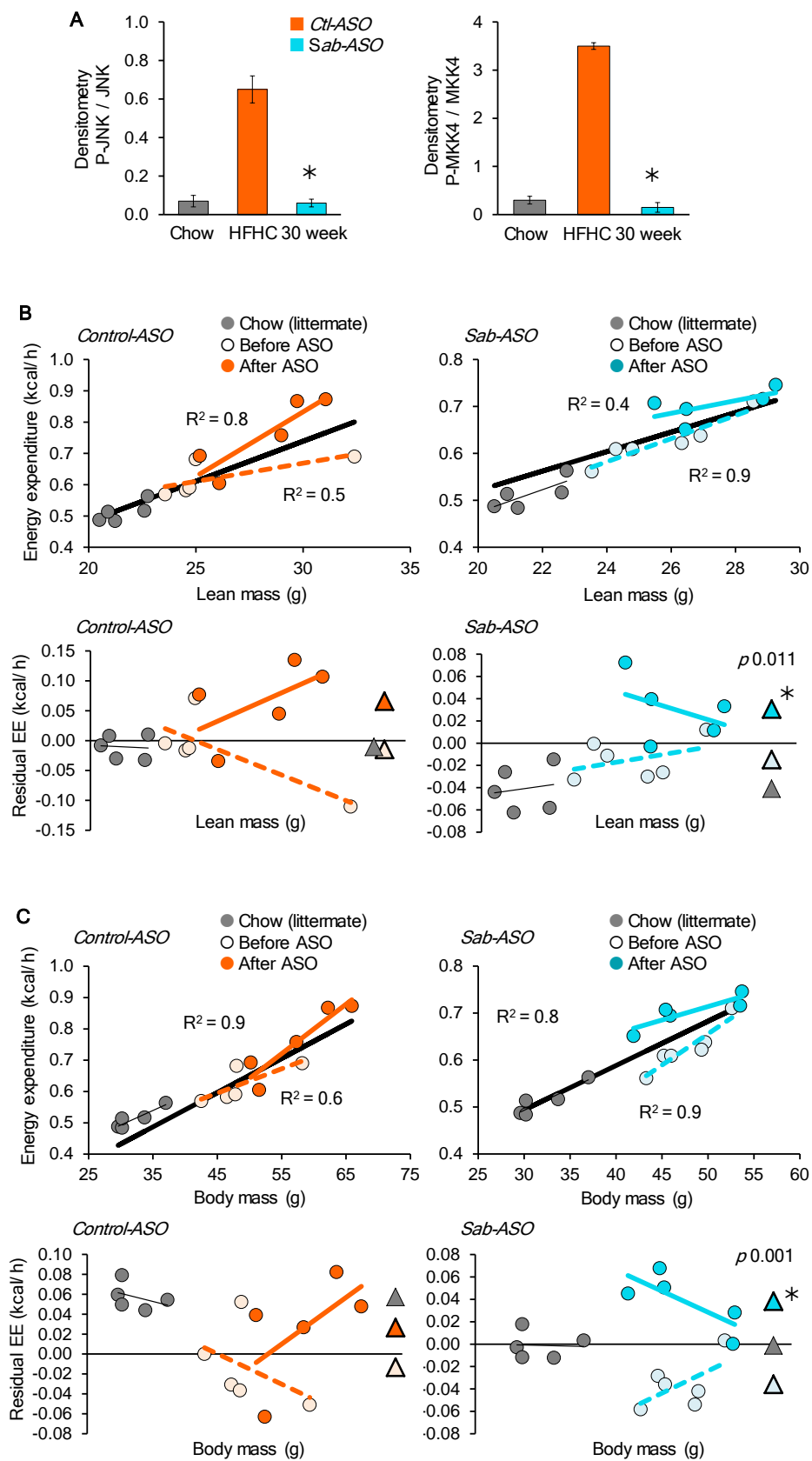
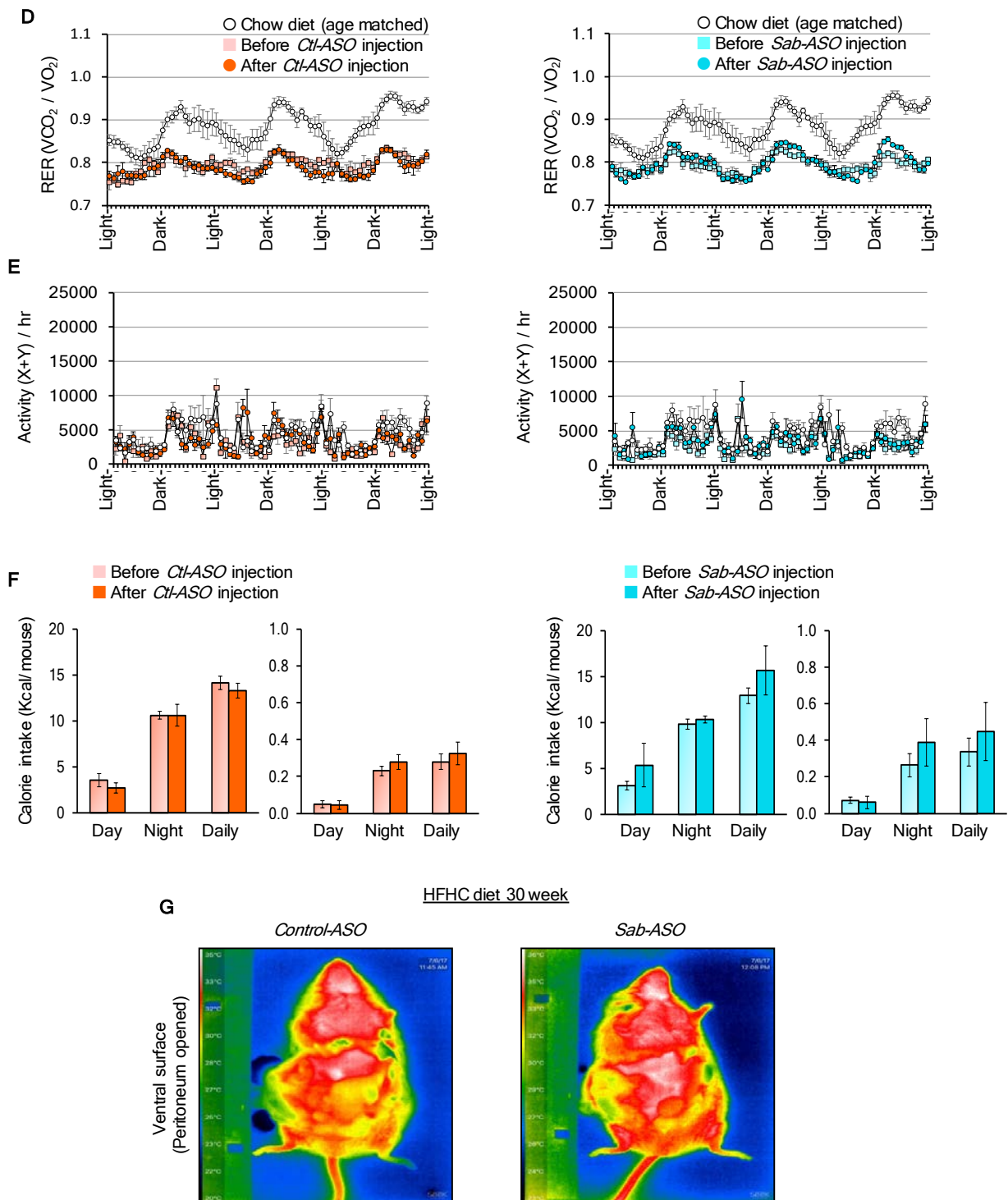


Fig. S5. Effect of Sab-ASO treatment on weight gain, hepatic steatosis, metabolic intolerance and SREBP activity.

(A-H) Wild type mice were fed the chow or HFHC diet for 15 weeks. High dose ASO (50mg/kg) to completely deplete SAB was given during the last 5 weeks of HFHC feeding. Mitochondrial SAB level (immunoblot), weight gain, body mass, hepatic steatosis (Oil Red O staining) and P-AKT/AKT (immunoblot), fasting glucose, GTT, OTT, and β -hydroxybutyrate were examined at the end of feeding. $n=5$ mice per group, $*=p<0.05$ Sab-ASO vs Ctl-ASO by unpaired, 2-tailed Student's *t*-test. (I) Liver mRNA expression of SREBP target genes after 30 weeks of HFHC diet feeding, control-ASO (Ctl-ASO) versus Sab-ASO (low dose 25mg/kg) treated mice were determined by qPCR. $*=p<0.05$, Sab-ASO vs Ctl-ASO by unpaired, 2-tailed Student's *t*-test. Data with SD represents average of 5 mice per group. (J) Representative liver histology of chow fed littermates at 30 weeks.

Figure S6





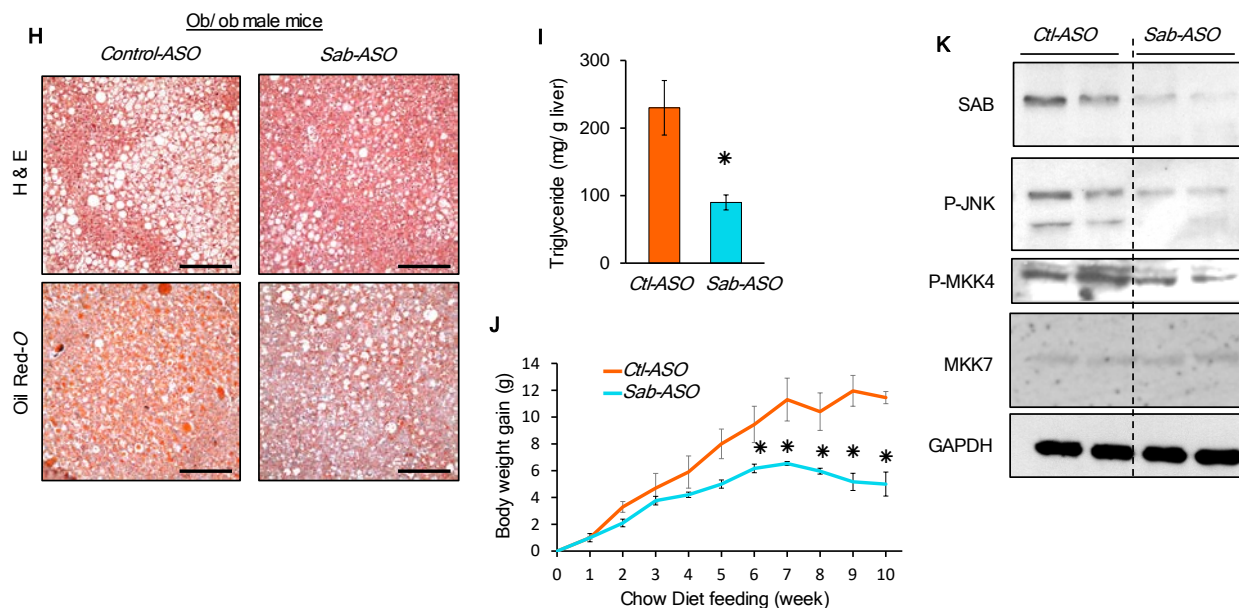
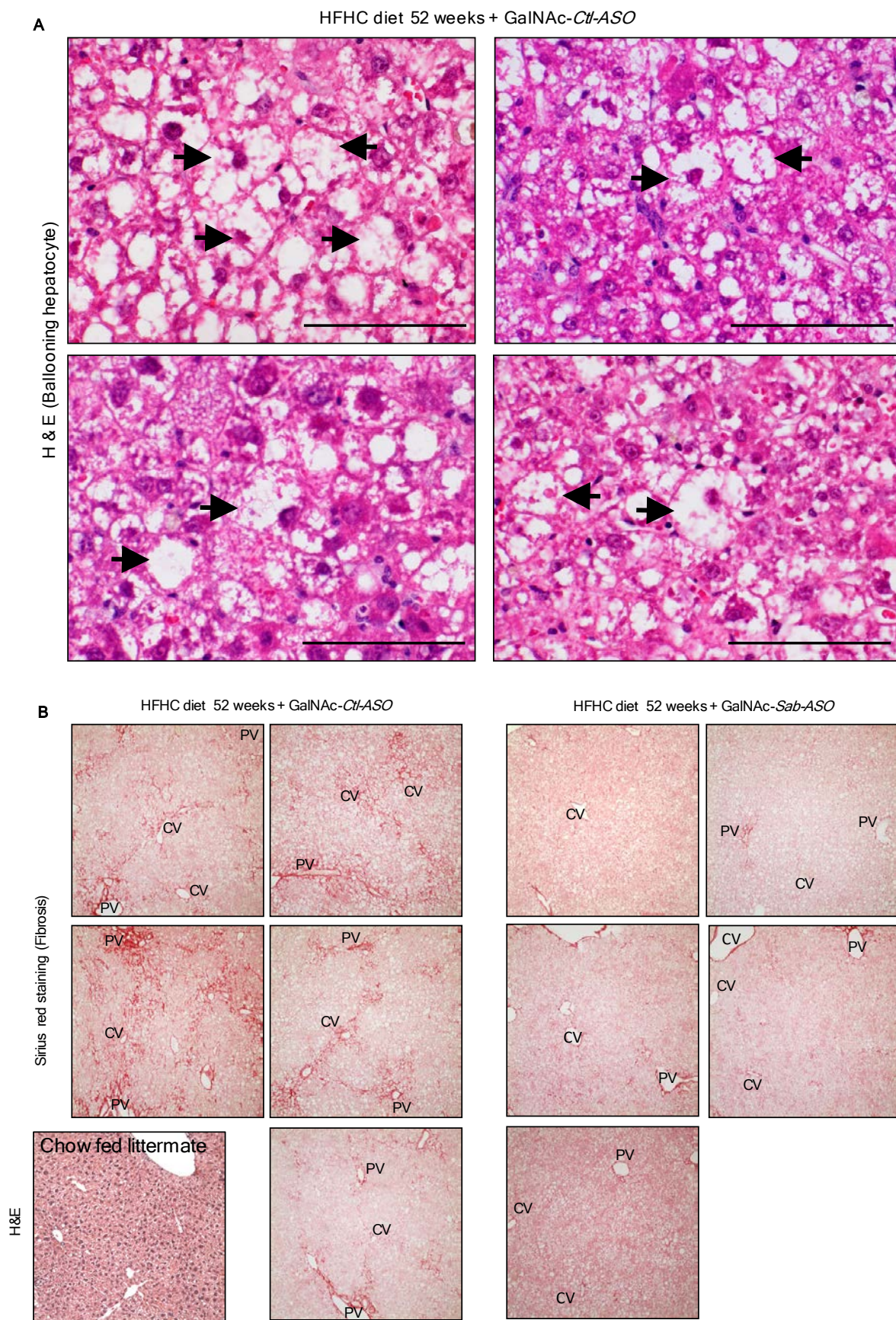
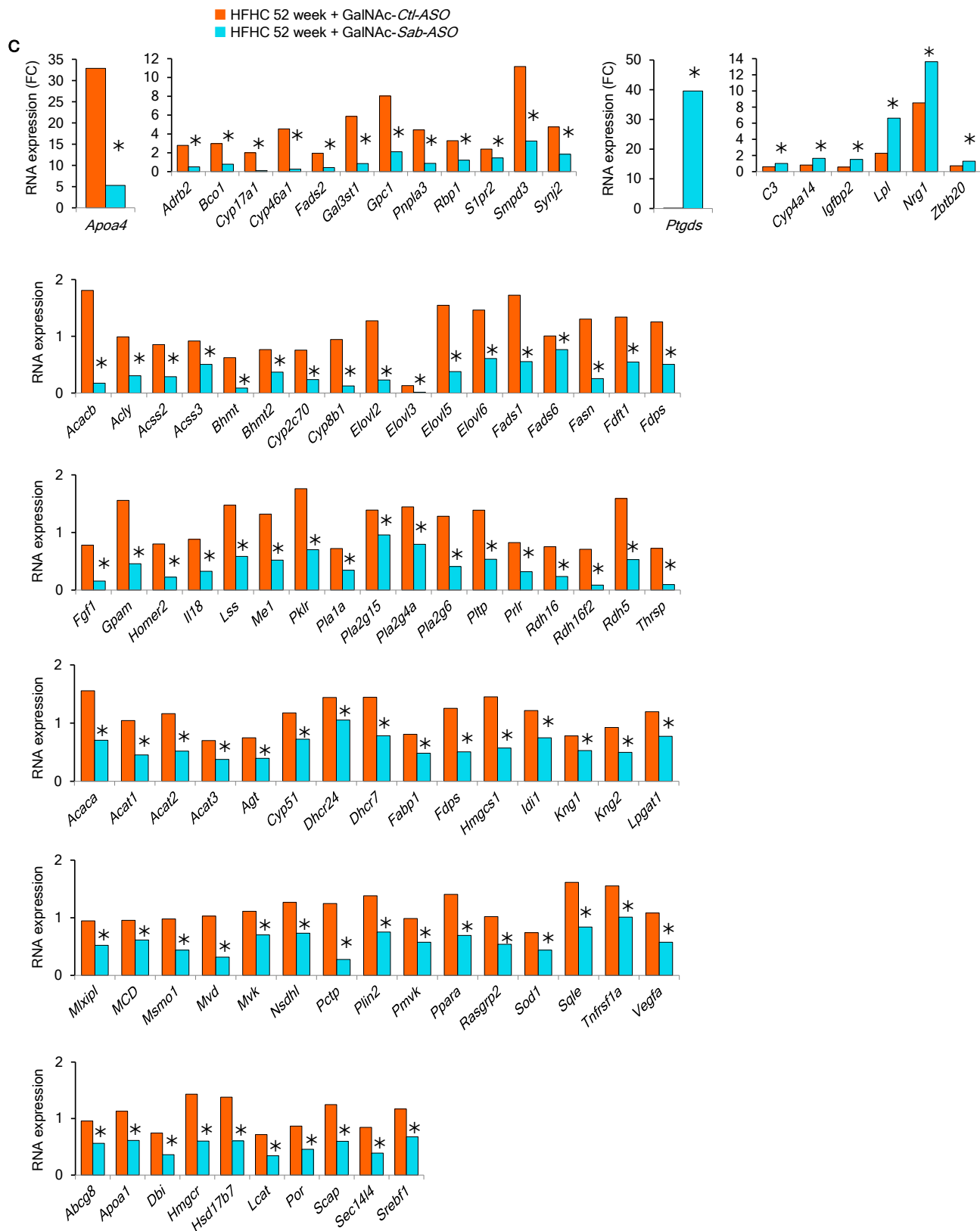


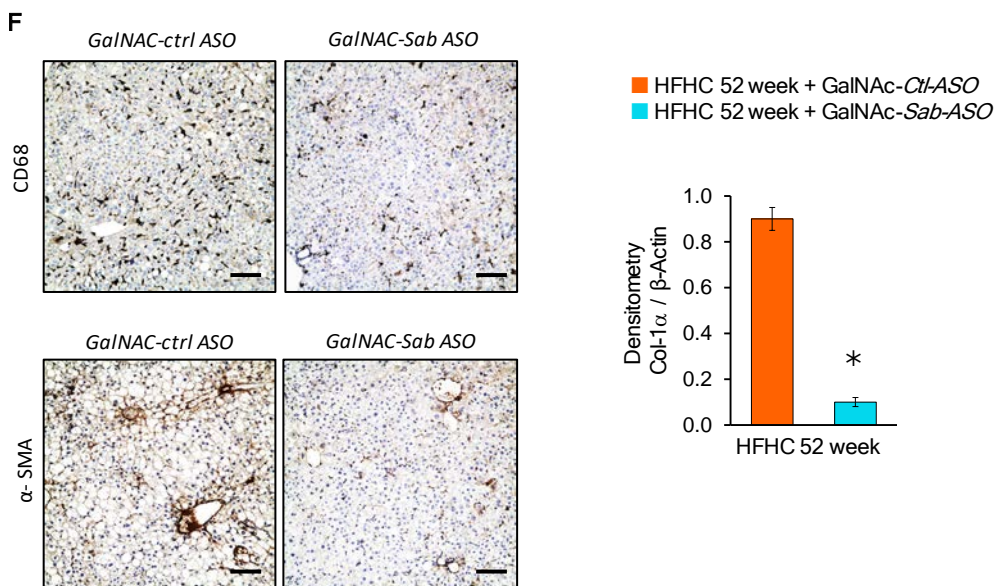
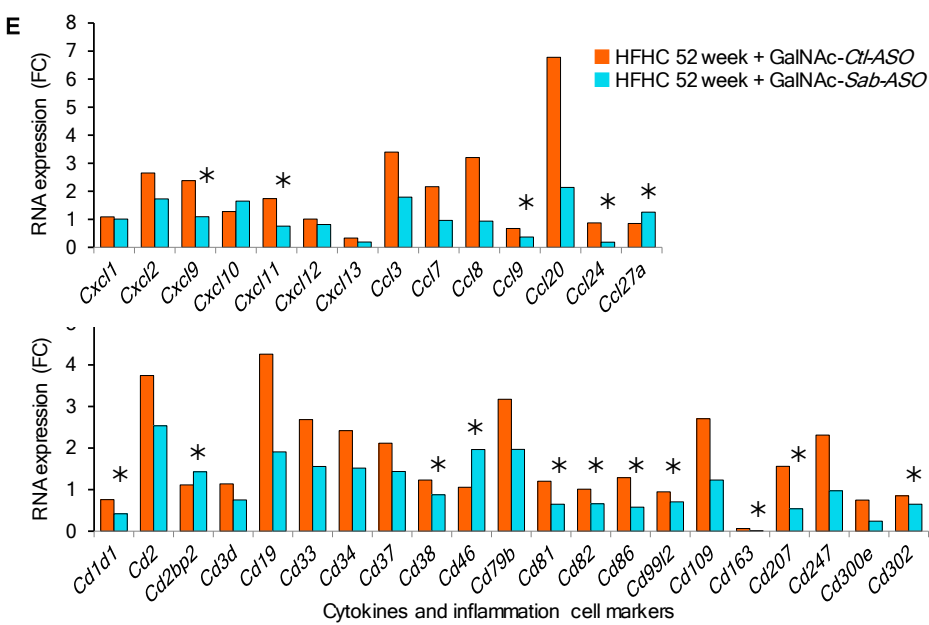
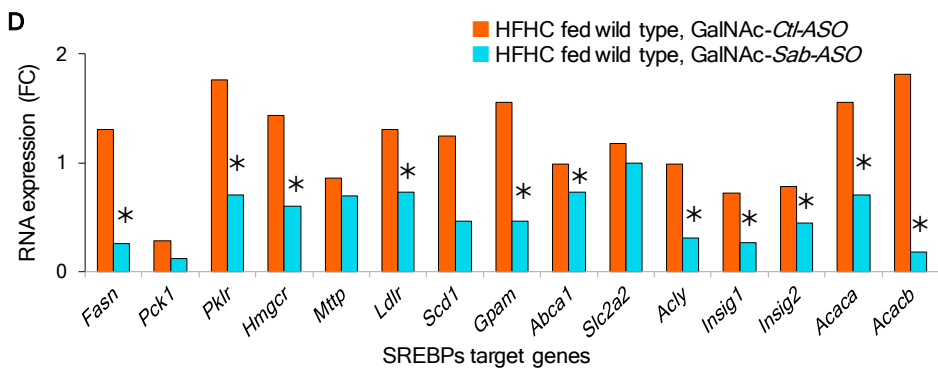
Fig. S6. Effect of Sab-ASO treatment on energy expenditure of mice fed HFHC diet for 30 weeks and Sab-ASO treatment of chow fed *ob/ob* mice. Male wild type littermates (at age 8 weeks) were fed HFHC diet for 30 weeks. Mice were given *Control-ASO* (*Ctl-ASO*) or *Sab-ASO* 25mg/kg intraperitoneally three times per week after 17 weeks of HFHC diet. Food and drink intake were not altered by the injections. **(A)** Densitometry of P-JNK / JNK and P-MKK4 / MKK4 measured on immunoblots of 3 separate experiments as in Fig 7A. n=4 mice/group. * = $p < 0.05$ *Sab-ASO* versus *Control-ASO* by unpaired, 2-tailed Student's *t*-test. All data are presented as mean \pm SEM. **(B-C)** Regression plots are depicted between energy expenditure (EE) vs lean mass or body mass of mice before and after ASO treatment. Residual EE obtained from regression plots were plotted with lean mass or body mass. Mean values of residuals of energy expenditure are shown as (Δ). Statistical significance of energy expenditure between after vs before ASO treatment is shown as (*) ($p < 0.05$, ANCOVA). n=5-6 mice per group. **(D-G)** Respiratory exchange ratio (RER), locomotor activity, calorie intake and body temperature of the mice were measured. Body heat was assessed using heat sensitive

thermal camera on the ventral surface (peritoneum opened) of anesthetized mice at room temperature. Surface temperature was estimated by color code from high to low: white, red, yellow, green, blue and black. Background blue color represents room temperature $\sim 23^{\circ}\text{C}$. **(H-K)** Chow fed *ob/ob* mice received *Control-ASO* or *Sab-ASO* for 10 weeks. Body weight was measured weekly. Liver fat accumulation was assessed by H&E and Oil-red-O staining as well as liver triglyceride measurement. Body weight gain **(J)** and P-JNK and P-MKK4 **(K)** were decreased in *Sab-ASO* compared to *Ctrl-ASO* treated group. $n=3$ mice per group $*=p<0.05$ *Sab-ASO* versus *Control-ASO* by unpaired, 2-tailed Student's *t*-test. Data represents mean \pm SEM

Figure S7







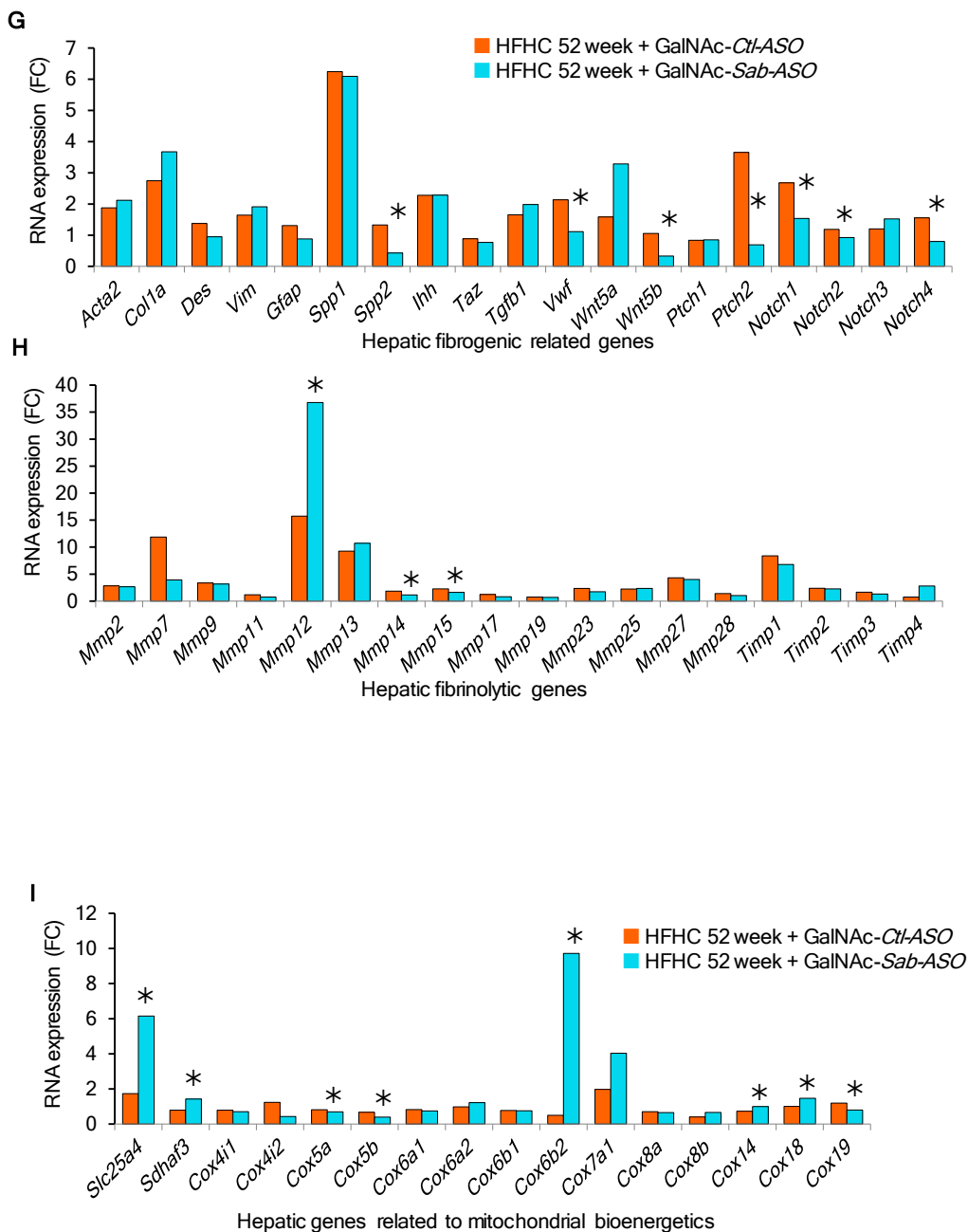


Fig. S7. Effect of hepatocyte targeted GalNAc-*Sab-ASO* treatment on NASH and liver metabolic pathways. Mice received GalNAc-*Control-ASO* or GalNAc-*Sab-ASO* for the last 10 weeks of 52 weeks of HFHC feeding. **(A)** high power magnification showing numerous ballooned hepatocytes (arrows) in GalNAc-*Control-ASO* treated mice. Representative images of individual mice treated with GalNAc-*Control-ASO*; Scale bar =

100 μm . **(B)** Sirius red stained photomicrograph from each mouse liver used for analysis of area of fibrosis in Fig.6 using Image-J. $n=5$ mice per group; 5-10 fields (10x magnification) per slide from each liver section. One representative liver histology from a 52 weeks chow fed littermate of the HFHC fed group shown on lower left **(C)** Differentially expressed gene (FDR < 0.05) fold change (FC) was obtained by RNA-seq analysis of GalNAc-*Control-ASO* and GalNAc-*Sab-ASO* treated HFHC diet fed mice for 52 weeks. Differential expression of genes related to triglyceride, fatty acid and cholesterol synthesis between GalNAc-*Control-ASO* and GalNAc-*Sab-ASO* treatment were identified by IPA analysis and are shown here. 88 out of 192 genes related to synthesis of triglyceride (overlap p -value $2.84\text{E-}20$) were changed, consistent with decreased synthesis of hepatic triglycerides (z-score = -4.322); 31 out of 71 genes related to synthesis of fatty acids (overlap p -value $2.43\text{E-}08$) were changed consistent with decreased synthesis of hepatic fatty acids (z-score = -2.377); 17 out of 44 genes related to synthesis of cholesterol (overlap p -value $5.08\text{E-}23$) were changed consistent with decreased synthesis of hepatic cholesterol (z-score = -2.642) by GalNAc-*Sab-ASO* versus GalNAc-*Control-ASO* treatment. $n=3$ mice per group; $*$ =FDR < 0.05, defined as significant FC difference between GalNAc-*Control-ASO* and GalNAc-*Sab-ASO* treatment. **(D)** Expression (FC) of SREBP 1 and 2 target genes was determined to assess SREBP activity. **(E)** Expression of genes related to hepatic expression of cytokine and inflammation in GalNAc-*Control-ASO* and GalNAc-*Sab-ASO* treated after 52 weeks of HFHC diet feeding. $*$ =FDR < 0.05, significant FC difference between GalNAc-*Control-ASO* and GalNAc-*Sab-ASO* treatment. $n=3$ per group. **(F)** Representative images of CD68 (macrophage) and α -SMA staining of liver histology of GalNAc-*Control-ASO* and GalNAc-*Sab-ASO* treated mice

after 52 weeks of HFHC diet feeding (n=3 mice/group). Bar graph shows densitometry of Col-1 α / β -Actin measured on immunoblots of 3 separate experiments from Fig 8G. n=5 mice/group. *= p <0.05 GalNAc-*Sab*-ASO versus GalNAc-*Control*-ASO by unpaired, 2-tailed Student's *t*-test. Data shown as mean \pm SEM. **(G-I)** Expression (FC) of genes related to hepatic expression of fibrogenesis and fibrinolysis, and mitochondrial bioenergetics in GalNAc-*Control*-ASO and GalNAc-*Sab*-ASO treated mice fed HFHC diet for 52 weeks is shown. *= FDR <0.05, significant FC difference between GalNAc-*Control*-ASO and GalNAc-*Sab*-ASO treatment. n=3 per group.

Figure S8

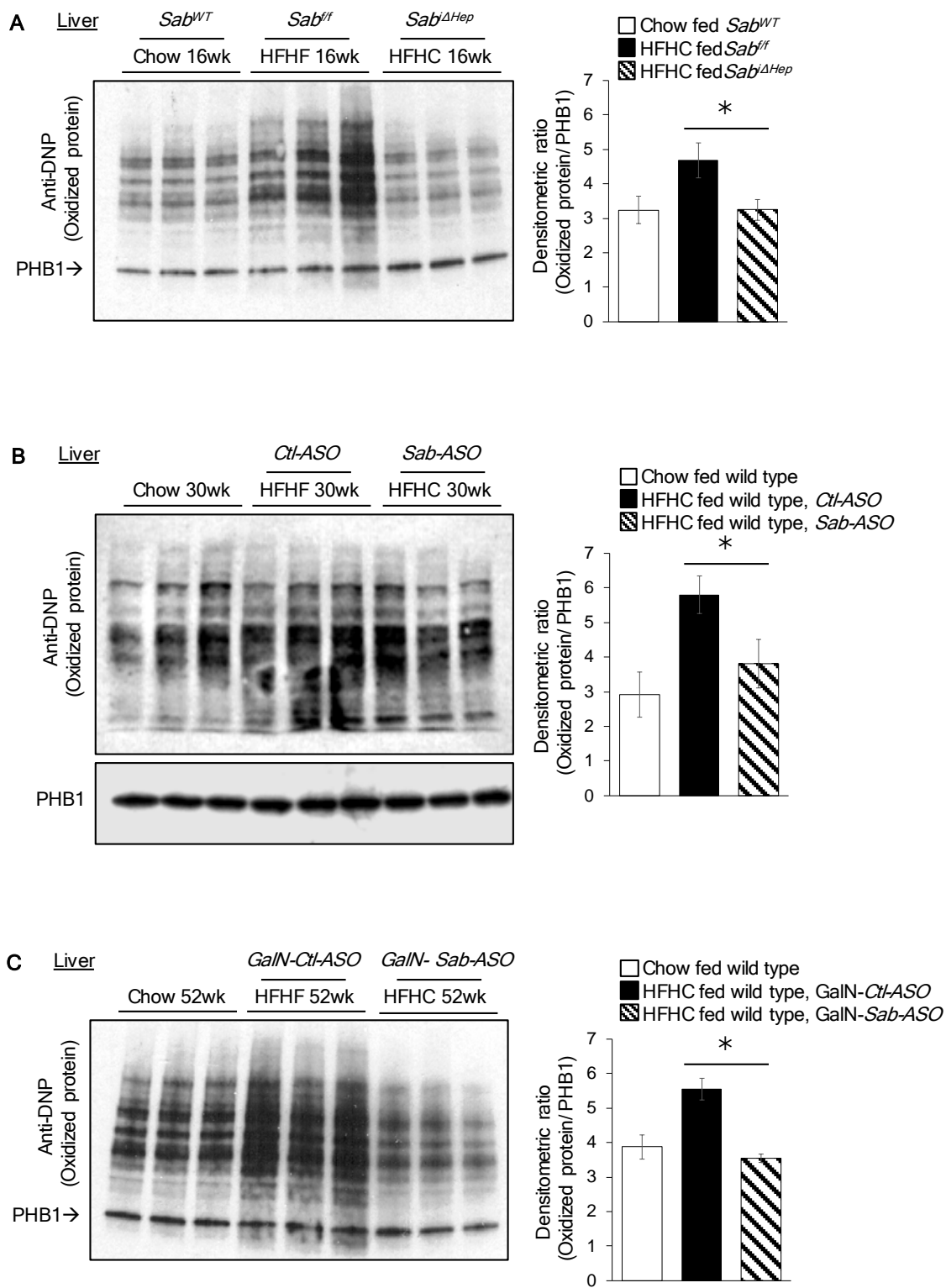


Fig. S8. Detection of oxidatively modified proteins in liver. Oxidatively modified proteins were detected by anti-dinitrophenylhydrazine (DNP) after derivatization of carbonyl groups in oxidized protein to DNP-hydrazone by reaction with 2,4-dinitrophenylhydrazine (DNPH). Oxidized proteins were separated and identified from a complex mixture by SDS-PAGE using 4-20% Tris-glycine gel. PHB1 is the loading control. (A, B, C) show dual detection of oxidized protein and PHB1. Each lane represents one mouse. Densitometric ratio of oxidized protein/PHB1 was determined. $*=p < 0.05$. $n=3$ mice per group, summarized by bar graphs. **(A)** 16 weeks Chow or HFHC diet fed Sab wild type (*Sab^{WT}*), *Sab^{ff}* or *Sab^{iΔHep}* mice. **(B)** The same 3 groups after 30 weeks and **(C)** after chow 52 weeks of feeding and treatment with *Sab*-ASO or GalN-*Sab*-ASO, respectively.